Comprehensive determination of the high–pressure structural behaviour of $BaTiO_3$

SUPPLEMENTARY INFORMATION

Craig L. Bull,[*,a,b] Christopher J. Ridley,[a] Kevin S. Knight,[c,d]
Nicholas P. Funnell[a] and Alexandra S. Gibbs[a,e]

[a] ISIS Neutron and Muon Facility, Rutherford Appleton Laboratory, Chilton, OX11 7XN, U.K.

[b] School of Chemistry, University of Edinburgh, David Brewster Road, Edinburgh EH9 3FJ, U.K.

[c] Department of Materials Science and Engineering, University of Sheffield, Sheffield S1 3JD, U.K.

[d] Department of Earth Sciences, The Natural History Museum, Cromwell Road, London, SW15 5BD, U.K.

[e] School of Chemistry, University of St Andrews, Fife, KY16 9SA, U.K.

[*]To whom correspondence should be addressed; E-mail: craig.bull@stfc.ac.uk

Submitted to Materials Advances

Table S1: Determined structural parameters from the refinement of $BaTiO_3$ upon compression at 480 K. Further structural details provided in the main text.Description of the goodness of fit parameters Rp, wRp and χ^2 are given in reference[S1]

Pressure (GPa)	Symmetry	a (Å)	V ($Å^3$)	Rp (%)	wRp (%)	χ^2
0.00(7)	Cubic	4.01259(6)	64.606(3)	7.35	6.13	0.87
0.08(7)	Cubic	4.01179(5)	64.568(3)	7.56	6.61	0.91
0.20(6)	Cubic	4.01084(7)	64.522(4)	7.87	6.53	0.96
0.41(7)	Cubic	4.00951(9)	64.458(4)	8.21	6.76	1.03
0.65(7)	Cubic	4.00735(11)	64.353(5)	8.23	7.01	1.09
0.99(8)	Cubic	4.00490(13)	64.235(6)	7.81	6.53	0.93
1.33(9)	Cubic	4.00113(13)	64.054(6)	6.70	5.56	1.34
1.79(1)	Cubic	3.99676(16)	63.844(7)	7.15	5.87	1.46
2.33(13)	Cubic	3.99168(16)	63.601(8)	6.68	5.66	1.34
3.19(16)	Cubic	3.9835(3)	63.212(12)	7.52	7.45	2.24
4.22(20)	Cubic	3.9743(2)	62.776(10)	6.31	5.31	1.10
4.98(23)	Cubic	3.9670(2)	62.429(11)	6.79	5.75	1.15

Table S2: Determined structural parameters from the refinement of $BaTiO_3$ upon compression at 290 K. Further structural details provided in the main text. Description of the goodness of fit parameters Rp, wRp and χ^2 are given in reference[S1]

Pressure (GPa)	Symmetry	a ($\AA$)	c ($\AA$)	V ($\AA^3$)	Ba(z)	O1(z)	O2(z)	Rp (%)	wRp (%)	χ^2
0.00(4)	Tetragonal	3.99423(8)	4.03501(10)	64.374(3)	0.478(6)	0.461(4)	-0.017(6)	4.35	4.06	0.7328
0.10(4)	Tetragonal	3.99291(8)	4.03330(16)	64.304(3)	0.474(5)	0.456(4)	-0.019(5)	4.68	4.21	0.6556
0.13(4)	Tetragonal	3.99265(10)	4.0322(2)	64.279(3)	0.481(7)	0.462(5)	-0.012(7)	5.98	5.16	0.6047
0.19(4)	Tetragonal	3.99255(9)	4.03172(19)	64.267(3)	0.461(5)	0.456(3)	-0.027(5)	5.71	5.01	0.5484
0.20(4)	Tetragonal	3.99225(9)	4.03066(19)	64.241(3)	0.475(5)	0.455(4)	-0.017(5)	5.94	5.41	0.617
0.27(4)	Tetragonal	3.99177(9)	4.03008(18)	64.216(3)	0.471(7)	0.463(5)	-0.019(6)	5.97	5.35	0.5906
0.40(5)	Tetragonal	3.99079(9)	4.02753(19)	64.144(3)	0.466(5)	0.460(4)	-0.026(5)	6.06	5.46	0.6058
0.56(4)	Tetragonal	3.98959(9)	4.0252(2)	64.069(3)	0.469(6)	0.461(4)	-0.024(6)	5.92	5.5	0.6062
0.68(5)	Tetragonal	3.98735(7)	4.02086(15)	63.927(2)	0.475(5)	0.464(4)	-0.015(5)	4.85	4.4	0.7294
0.94(5)	Tetragonal	3.98632(7)	4.01881(15)	63.862(2)	0.480(6)	0.467(4)	-0.013(5)	4.13	4.02	0.9349
1.08(5)	Tetragonal	3.98568(8)	4.01725(16)	63.817(2)	0.495(7)	0.476(6)	-0.001(6)	4.77	4.34	0.7393
1.15(6)	Tetragonal	3.98482(8)	4.01660(18)	63.779(3)	0.487(5)	0.472(6)	-0.006(7)	4.93	4.61	0.7387
1.37(6)	Tetragonal	3.98323(8)	4.01350(17)	63.679(2)	0.479(7)	0.469(5)	-0.011(7)	5.41	5.06	0.8672
1.59(6)	Tetragonal	3.98178(8)	4.00970(16)	63.572(2)	0.488(7)	0.475(5)	-0.003(7)	4.26	4.01	1.067
1.82(7)	Tetragonal	3.98019(8)	4.00530(17)	63.451(2)	0.487(9)	0.476(6)	-0.004(8)	4.24	4.03	1.054
2.07(7)	Tetragonal	3.97829(8)	4.00123(17)	63.327(2)	0.493(11)	0.486(8)	-0.004(8)	4.447	4.08	1.05
2.2(7)	Tetragonal	3.97707(10)	3.9985(2)	63.245(3)	0.483(9)	0.472(6)	-0.010(8)	5.1	4.73	0.7375
2.55(8)	Tetragonal	3.97537(12)	3.9930(2)	63.104(3)	0.481(10)	0.478(9)	-0.006(9)	5.39	4.75	0.7767
2.83(9)	Cubic	3.97790(5)	-	62.944(2)	-	-	-	5.08	4.66	0.9616
3.14(9)	Cubic	3.97499(5)	-	62.807(2)	-	-	-	4.76	4.39	1.115
3.44(10)	Cubic	3.97235(5)	-	62.682(3)	-	-	-	5.6	5.05	0.7245
3.80(11)	Cubic	3.96921(5)	-	62.534(2)	-	-	-	5.01	4.98	1.24
4.22(12)	Cubic	3.96654(6)	-	62.407(3)	-	-	-	6.26	5.86	0.8923
4.68(13)	Cubic	3.96279(5)	-	62.231(2)	-	-	-	5.41	5.06	0.9696
5.07(14)	Cubic	3.95970(5)	-	62.085(3)	-	-	-	5.57	5.25	1.019
5.84(16)	Cubic	3.95384(6)	-	61.810(3)	-	-	-	5.81	5.35	1.003

Table S3: Determined structural parameters from the refinement of $BaTiO_3$ upon compression at 225 K. Further structural details provided in the main text. Description of the goodness of fit parameters Rp, wRp and χ^2 are given in reference[S1]

Pressure (GPa)	Symmetry	a (Å)	b (Å)	c (Å)	V (Å^3)	Ba(z)	O1(z)	O2(x)	O2(z)	Rp (%)	wRp (%)	χ^2
0.00(4)	Orthorhombic	5.6745(6)	3.98496(17)	5.68806)	128.623(6)	0.027(4)	0.013(6)	0.258(3)	0.275(4)	5.25	4.19	1.003
0.01(4)	Orthorhombic	5.6740(5)	3.9848(2)	5.6889(5)	128.627(8)	0.020(8)	0.020(8)	0.257(4)	0.277(6)	6.51	5.47	0.658
0.06(4)	Orthorhombic	5.6733(5)	3.9856(2)	5.6876(6)	128.607(8)	0.028(4)	0.025(7)	0.258(3)	0.276(7)	6.9	5.91	0.5459
0.02(4)	Orthorhombic	5.6738(4)	3.9845(2)	5.6876(5)	128.583(7)	0.026(4)	0.012(7)	0.256(3)	0.276(5)	5.9	4.93	0.6996
0.2594)	Orthorhombic	5.6699 (4)	3.98389(19)	5.6829(5)	128.367(7)	0.032(3)	0.011(5)	0.250(2)	0.273(6)	5.69	4.63	0.8678
0.51(4)	Orthorhombic	5.6650(6)	3.9812(2)	5.6775(5)	128.047(7)	0.027(4)	0.015(7)	0.259(4)	0.273(7)	5.68	4.63	0.8609
0.64(4)	Orthorhombic	5.6628(10)	3.9810(2)	5.6720(10)	127.871(7)	0.021(7)	0.009(8)	0.259(3)	0.270(6)	5.44	4.54	0.8247
0.75(4)	Orthorhombic	5.6619(10)	3.9800(2)	5.6713(10)	127.801(7)	0.023(8)	0.008(8)	0.259(4)	0.272(8)	5.58	4.61	0.853
0.90(4)	Orthorhombic	5.6600(13)	3.9793(2)	5.6670(14)	127.640(7)	0.023(12)	0.006(9)	0.255(5)	0.271(9)	5.75	4.6	0.8363
1.05(4)	Orthorhombic	5.6570(13)	3.9789(2)	5.6640(13)	127.488(7)	0.017(9)	-0.001(1)	0.259(4)	0.265(9)	5.58	4.47	0.8467
1.22(5)	Orthorhombic	5.6534(10)	3.97728(19)	5.6613(10)	127.296(10)	0.017(9)	0.006(8)	0.257(4)	0.266(8)	4.66	3.71	2.158
1.49(5)	Orthorhombic	5.652(3)	3.9755(2)	5.655(3)	127.068(6)	0.006(10)	-0.007(9)	0.259(3)	0.256(8)	5	4.08	1.291
1.77(5)	Orthorhombic	5.648(3)	3.9737(2)	5.646(3)	126.749(6)	-0.005(10)	-0.008(8)	0.264(2)	0.236(7)	5.04	4	2.157
2.172	Mixed											
2.69(7)	Tetragonal	3.96763(13)	- -	3.9847(3)	62.728(3)	0.519(14)	0.505(16)	-	0.022(12)	6.08	507	0.9318
3.84(9)	Tetragonal	3.96308(16)	-	3.9759(3)	62.446(3)	0.551)10)	0.534(14)	-	0.040(14)	5.57	4.75	1.495
4.45(10)	Tetragonal	3.9586(2)	-	3.9687(5)	62.194(3)	0.536(13)	0.518(2)	-	0.031(11)	6.32	5.2	0.9339
			- -									
5.03(11)	Tetragonal	3.95453(19)	-	3.9643(4)	61.996(3)	0.539(7)	0.56(14)	-	0.028(9)	6.2	5.24	0.9259
5.03(11)	Cubic	3.95763(7)	- -	-	61.988(3)	-	-	-	-	6.24	5.24	0.9231
			- -									
5.75(13)	Cubic	3.95159(7)	-	-	61.704(3)	-	-	-	-	5.77	4.6 1.38	

Table S4: Determined structural parameters from the refinement of $BaTiO_3$ upon compression at 175 K. Further structural details provided in the main text. Description of the goodness of fit parameters Rp, wRp and χ^2 are given in reference[S1]

Pressure (GPa)	Symmetry	a(Å)	$\alpha(^\circ)$	V ($Å^3$)	Ba(x)	O1(x)	O1(y)	Rp (%)	wRp (%)	χ^2
0.0(3)	Trigonal	4.05588(8)	90.02(4)	64.234(4)	0.517(3)	0.007(3)	0.522(4)	4.2	3.85	1.35
0.36(4)	Trigonal	4.00134(9)	90.98(3)	64.065(4)	0.515(3)	0.003(3)	0.511(4)	3.9	3.74	1.27
0.63(4)	Trigonal	3.99900(9)	90.10(4)	63.952(4)	0.513(3)	-0.005(3)	0.514(3)	3.8	3.7	1.22
0.91(4)	Trigonal	3.99606(10)	90.05(9)	63.811(5)	0.514(4)	0.004(4)	0.515(6)	4	3.8	1.27
1.24(5)	Trigonal	3.99235(9)	90.06(2)	63.633(4)	0.515(3)	0.004(4)	0.516(6)	4	3.6	1.87
1.61(5)	Trigonal	3.98872(10)	90.028(16)	63.460(5)	0.514(4)	0.002(4)	0.514(7)	4.4	3.8	1.96
2.50(4)	Trigonal	3.97913(11)	90.05(3)	63.004(5)	0.506(13)	-0.001(15)	0.513(11)	4.5	3.8	1.22

Pressure (GPa)	Symmetry	a(Å)	b(Å)	c(Å)	V ($Å^3$)	Ba(z)	O1(z)	O2(x)	O2(z)	Rp	wrP	χ^2
3.60(5)	Orthorhombic	5.622(7)	3.9522(6)	5.625(7)	124.982(13)	-0.009(6)	-0.034(6)	0.249(3)	0.226(5)	4.7	3.9	1.23
4.70(6)	Orthorhombic	5.561(10)	3.9379(1)	5.607(10)	123.884(15)	-0.019(6)	-0.027(5)	0.257(4)	0.219(4)	4.6	3.8	1.10

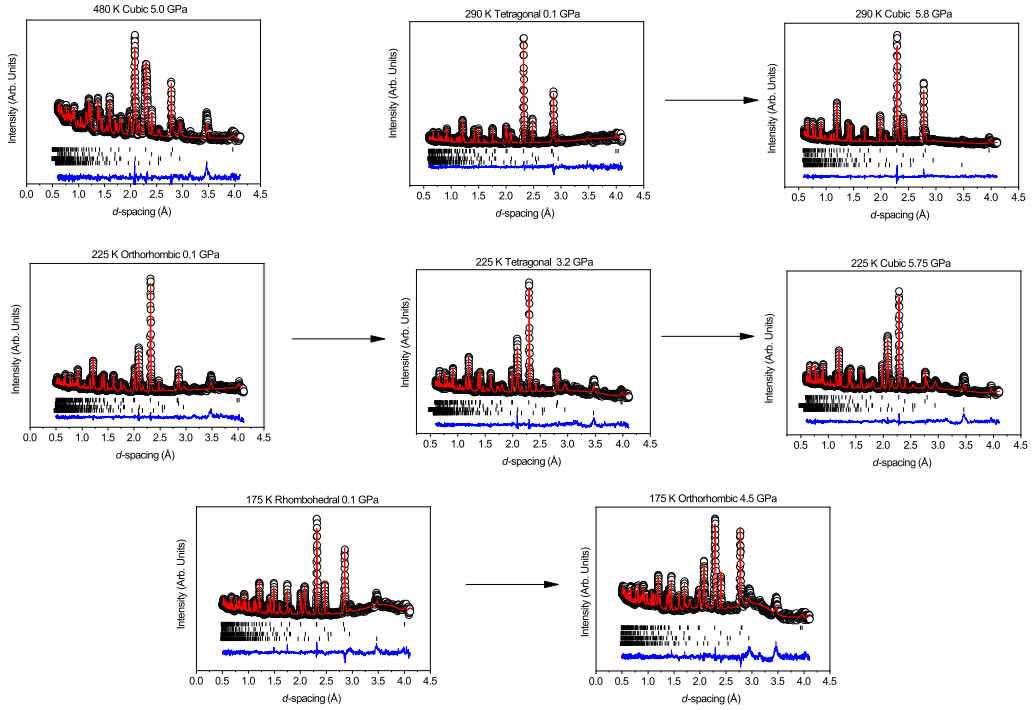

Figure S1: Representative neutron diffraction patterns of $BaTiO_3$ as a function of pressure and temperature. In each diffraction pattern the data are represented by open circles, the Rietveld fit by the solid red line and the residual by the blue trace. The vertical bars indicate the expected positions of reflection and from top to bottom in each panel represents $BaTiO_3$, lead, ZrO_2 and Al_2O_3 respectively. In the region at high d-spacing often the strained anvils lead to a misfitting (and hence high residual) and at lower temperatures the pressure transmitting medium can result in an amorphous background which is more problematic to fit.

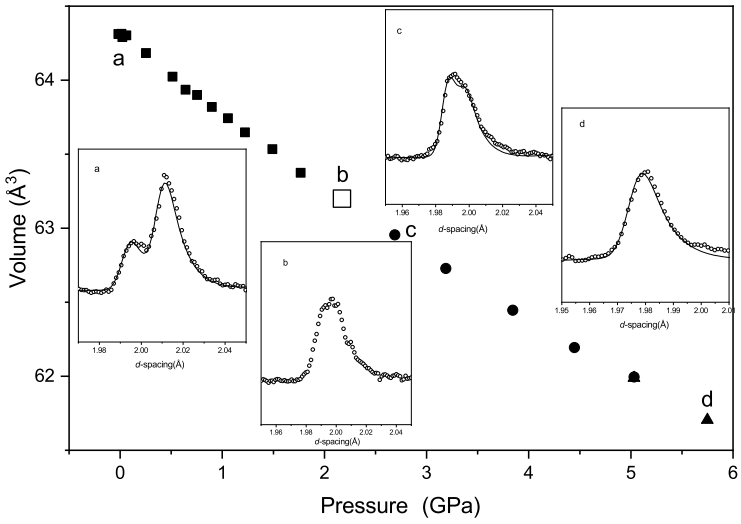

Figure S2: Variation in unit cell volume per formula unit for $BaTiO_3$ at 225 K. The solid squares are for the orthorhombic phase. The open square symbol represents the mixed phase point (orthorhombic and tetragonal). The solid circles the tetragonal phase and the solid trianghle the cubic phase. The inserts show the region around the diagnostic reflections observed around $\sim$2 Å, and the letters for each insert panel show region in compression curve from where they were measured.

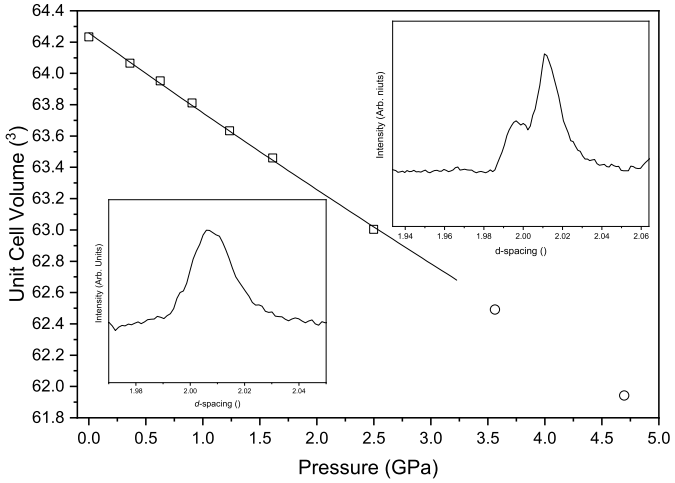

Figure S3: Variation in unit cell volume per formula unit for $BaTiO_3$ at 175 K. The open squares are for the rhombohedral phase. The open circle symbols represent the orthorhombic phase. The solid line is the second order Birch-Murnaghan equation of state fit to the rhombohedral phase. The bottom left insert shows the diffraction pattern of the rhombohedral phase close to ambient pressure at 175 K around the 200 reflection. The top right insert shows the diffraction pattern of the orthorhombic phase at ambient pressure at 225 K in the region of the 020/202 reflections.

1 Spontaneous Strain Determination

The lattice parameters for the tetragonal and orthorhombic phases have been converted into spontaneous strains relative to the cubic phase. This has been performed in accordance to that described by Hayward *et al.*[S2] In the tetragonal phase there is a tetragonal strain (e_t) and defined by

$$e_t(z) = \frac{1}{\sqrt{3}}(2e_3 - e_1 - e_2) = \frac{1}{\sqrt{3}}\left(\frac{c-a'}{a'} - \frac{a-a'}{a'}\right)$$

(1)

where a' is defined as the value of the cubic lattice parameter would have at the pressure and temperature in the absence of the phase transition. At 290 K this can be determined by extrapolation of the variation of the a lattice parameter in the cubic phase from 2.6–5.8 GPa (as suggested by Carpenter *et al*).[S3] This extrapolation of the cubic lattice parameter and the variation in the tetragonal strain at 290 K for the tetragonal phase is shown in Figure S5.

In the orthorhombic phase there is tetragonal strain (e_t), with a principal axis parallel to to the x_0 crystallographic direction and is defined as

$$e_t(x) = \frac{1}{\sqrt{3}}(2e_1 - e_2 - e_3) = \frac{1}{\sqrt{3}}\left(2\frac{b-a'}{a'} - \frac{\frac{a}{\sqrt{2}}-a'}{a'} - \frac{\frac{c}{\sqrt{2}}-a'}{a'}\right) \quad (2)$$

there is also a shear strain e_4 and is defined as

$$\mid e_4 \mid = \frac{\frac{a}{\sqrt{2}}-a'}{a'} - \frac{\frac{c}{\sqrt{2}}-a'}{a'} \quad (3)$$

However, at 225 K there is not sufficient data to extrapolate from the two cubic data points at 5 and 5.7 GPa the cubic behaviour in the tetragonal and orthorhombic phase. As a result at 225 K the spontaneous strains $e_t(x)$ and e_4 have been determined on the basis that transitions have no volume strain and $a' = \sqrt{[}3]V$. A test of this methodology was performed on the tetragonal phase at 290 K and the variation in $e_t(x)$ is only seen in the fourth decimal point when comparing the methods of obtaining a'. On this basis the variation of the tetragonal strain for the orthorhombic and tetragonal phase at 225 K with pressure is potted in Figure S5 and as well as e_4 for the orthorhombic phase. For the rhombohedral phase it is not possible to determine the strain - this is as a result that the in the unit cell angle is very close to 90° and hence the strain is very close to if not zero. A measurement of this small distortion is also instrument resolution limited and the PEARL instrument is only a medium resolution instrument. A general increase in the rhombohedral cell angle is observed with increasing pressure although relatively small.

2 References

(S1) B. H. Toby, *Powder Diffraction*, 2006, **21**, 67–70.

(S2) S. A. Hayward, S. A. T. Redfern, H. J. Stone, M. G. Tucker, K. R. Whittle and W. G. Marshall, *Zeitschrift für Kristallographie - Crystalline Materials*, 2005, **220**, 739–739.

(S3) M. A. Carpenter, E. K. Salje and A. Graeme-Barber, *European Journal of Mineralogy*, 1998, **10**, 621–691.

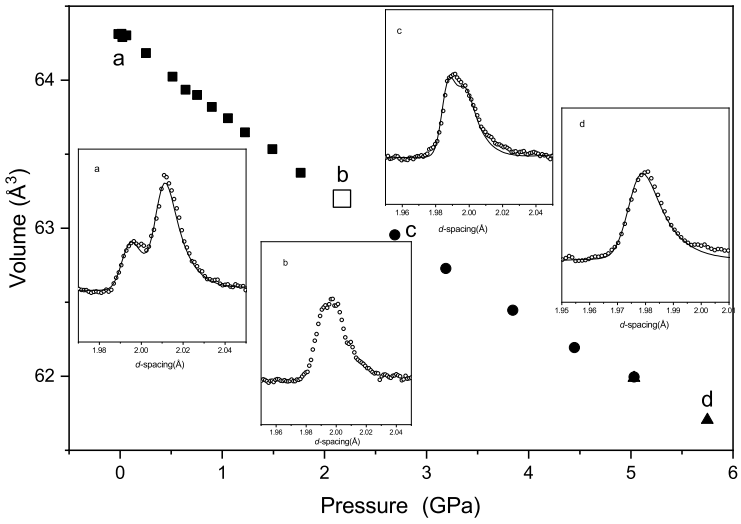

Figure S4: Variation in unit cell volume per formula unit for $BaTiO_3$ at 225 K. The solid squares are for the orthorhombic phase. The open square symbol represents the mixed phase point (orthorhombic and tetragonal). The solid circles the tetragonal phase and the solid trianghle the cubic phase. The inserts show the region around the diagnostic reflections observed around $\sim$2 Å, and the letters for each insert panel show region in compression curve from where they were measured.

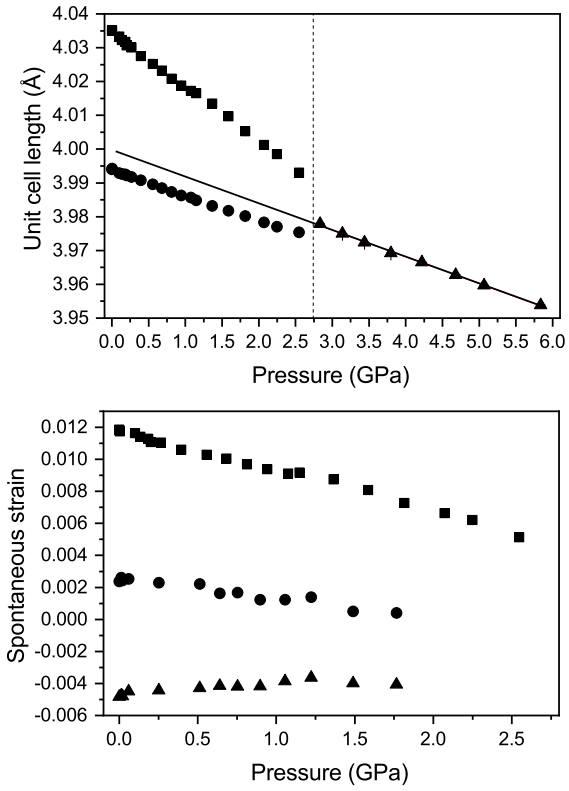

Figure S5: Top: Variation in lattice parameters of $BaTiO_3$ with increasing pressure at 290 K. The solid squares and circles show the value of the a and c lattice parameters of the tetragonal phase and the solid triangles the cubic lattice parameter. The solid line a fit to the cubic lattice parameter variation with pressure and the linear fit is used to determine the expected cubic lattice parameter at lower pressure in the absence of a phase transition. Bottom: Variation in spontaneous strain in $BaTiO_3$ with increasing pressure. The tetragonal ($e_t(z)$) strain in the tetragonal phase at 290 K is shown as solid squares ($e_t(x)$) and for the orthorhombic phase at 225 K as solid circles. The shear strain (e_4) in the orthorhombic phase at 225 K is shown as solid triangles.